Technical Design Report for the 2021 Collegiate Wind Competition

Wildcat Wind Power

Kansas State University

Electrical Team
Matthew Monsion (Electrical Team Lead)
Hayden Dillavou (Vice President)
Michael Brosseit
Tyler Schooley
Brianna Wagoner
Jose Mateus Raitz
Patrick Flett
Robert Foeller

Mechanical Team
Kavian Kalantari (Vice President)
Eric Christman (President)
Bryce Rogers (Mechanical Team Co-Lead)
Luke Price (Mechanical Team Co-Lead)
Adam Reelfs
Jett Bendure
Stephen Kielhofner
Wesley Smith
Josh Meurer
Chase Eccles

Advisors
Dr. Warren White – KSU Mechanical and Nuclear Engineering
Dr. Hongyu Wu – KSU Electrical and Computer Engineering

Contact:
Eric Christman - President - echris018@ksu.edu
Dr. Warren White - Advisor - wnw@ksu.edu

Table of Contents

Chapter 1 – Executive Summary

This competition year, the turbine design team had the goal of redesigning many turbine control systems and improving performance in the safety and regulation tasks that they have struggled with in the past. Additionally, the team aimed to test new blade and motor designs in order to improve cut-in and power curve performance. The final turbine was a 3-bladed, fixed pitch, direct drive assembly, with a passive centrifugal RPM control system in addition to a variable resistance load.

The blades selected for the turbine were similar to blades used in past designs, and incorporated the SA7024 and BE50sm airfoils. For the generator, the team tested a variety of generator models, and settled on a Tarot 4114 320KV design given that it produced relatively high power at lower wind speeds. This combination did lead to strong power production at wind speeds above 7 m/s, but the turbine cut-in wind speed remained above the 5 m/s mark.

To regulate turbine RPM, many passive centrifugal brake styles were evaluated, and the team settled on a design that actuates through outward flexing of a 3D-printed brake shoe against a similarly constructed drum. This design was chosen due to its ease of construction, replacement, and modification of parameters. Connection of the rotating brake module to the driveshaft required the fabrication of a keyed driveshaft, which the team succeeded in procuring and modifying. The final brake design successfully regulated RPM during testing, but the team did struggle to get the system to activate at the correct RPM value.

To regulate and optimize turbine power output, the team worked to design a variable resistance load. This effort was successful, and the final load had relatively fine resistance control between 0 and 16 Ω. The resistances chosen were in the range of the optimal resistance for the generator, and the overall design allowed for accurate and fast power regulation.

Regulating and optimizing power through the variable resistance load required the collection of data from sensors to estimate wind speed, from which optimal power resistances were determined. The team developed isolated communications between microcontrollers on both sides of the PCC, which allowed for RPM data to be sent to the load. These communication lines were also used to trigger and execute safety braking procedures.

The operation of the entire turbine system was dictated by the microcontroller in the load, which collected data from sensors and calculated an operational state through equations obtained from testing data. The load could choose to optimize power if it calculated a wind speed less than 11 m/s, or regulate power if it calculated a wind speed greater than 11 m/s. The centrifugal brake, being a completely passive mechanism, required no actuation from a microcontroller to operate. The load also had the ability to execute cut-in procedures at low wind speeds, and enact braking procedures if it detected changes in the braking switch positions or a disconnection at the PCC.

Chapter 2 – Mechanical Design

2.1 Design Objective

The mechanical design objectives for the team included the design of a new RPM control mechanism, as well as improved nacelle design through better control of manuf acturing tolerances. Additionally, the team aimed to streamline manufacturing processes to allow for rapid testing of new components in the nacelle. Given the distributed design and manufacturing environment for much of the competition year, the team elected not to make serious changes to blade design from previous turbines, and instead focus on RPM regulation. The team has not managed to design effective RPM regulation systems in the past, making it an important design focus for this year's competition.

2.2 Blade Design

Previous members of the Wildcat Wind Power team developed an in-house Python program to compare thousands of airfoils at multiple locations along the span of the blade. The airfoils with the highest lift and lowest drag for each section of the blade were then chosen. The resulting blade design consisted of the thin, high lift, low drag SA7024 and BE50sm airfoils. Q-Blade was then used to further optimize the design by adding a 30 degree twist along the span of the blade. The team's blades were then 3D printed with highest quality settings on a Prusa i3 MK3.

2.3 Blade Analysis

With the final blade design selected, it must be analyzed to ensure that it will perform safely in the high wind speed environment of the wind tunnel during testing. SolidWorks finite element analysis simulation tools were utilized to analyze the stresses on the blades and determine if failure would occur.

There are two forces that generate stress on the blades: the centripetal force as a result of the rotation of the hub, and the force of the wind pushing on the top surface of the blades. The centripetal forces acting on the blade are the most significant. At wind speeds of about 12.5 m/s, the team found through wind tunnel testing that the blades rotate at approximately 4300 RPM when the turbine is unloaded. To apply the centrifugal force as well as the necessary constraints to the SolidWorks simulation, an adapter inspired by the centrifuges used to train military pilots and astronauts was created to represent the actual axis of rotation about the drive shaft:

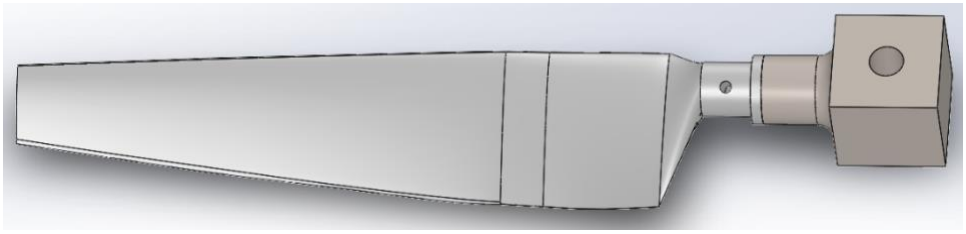

Figure [1]: Blade-adapter assembly

The blade and the adapter are bonded in the simulation to ensure the two parts have no way of separating from one another.

The force of the air pushing on the blade is also needed to form a complete stress analysis of the blade. The force of wind at 12.5 m/s on the blade was calculated with the following equation:

$$F_{wind} = \frac{1}{2}\rho_{air} A_s v^2 = \frac{1}{2}(1.225\ \frac{kg}{m^3})(0.006529\ m^2)(12.5\ \frac{m}{s})^2 = 0.625\ N$$

In the simulation this force was modeled as being uniformly distributed across the entire top surface of the blade. Split lines were added to the leading and trailing edges of the blade to separate the top and bottom surfaces so the load could be applied to just the top surface. The following figure shows the applied forces and boundary conditions:

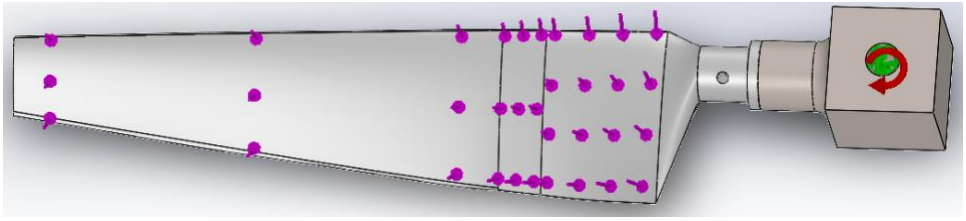

Figure [2]: Applied loads and constraints

Extremely fine mesh controls were added at locations where stress concentrations were expected. Testing has shown that when blades fail, they almost always do so at the plane where the loft that connects the root to the airfoil meet. A mesh control was also added to the blade tip to ensure that the blade's mesh would always have a minimum of two elements in the thickness direction.

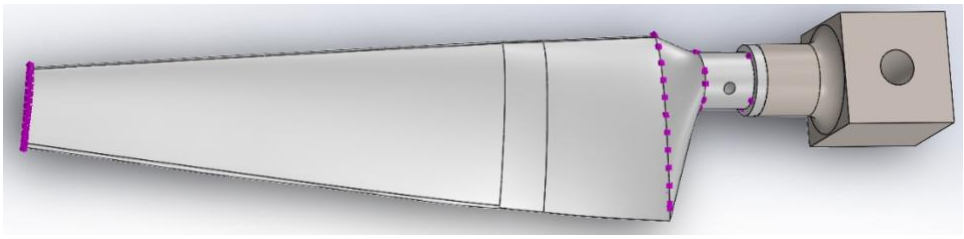

Figure [3]: Mesh control locations

The blades are 3D printed using PLA. SolidWorks does not have a predefined PLA material, so a custom material was defined using the mechanical properties sourced from a paper by MIT [1]:

Property	Value	Units
Elastic Modulus	3500000000	N/m^2
Poisson's Ratio	0.36	N/A
Shear Modulus	1287000000	N/m^2
Mass Density	1252	kg/m^3
Tensile Strength	59000000	N/m^2
Compressive Strength		N/m^2
Yield Strength	70000000	N/m^2
Thermal Expansion Coefficient		/K

Figure [4]: Mechanical Properties of PLA used in FEA Simulation

After running the simulation, the following stress concentrations were revealed at the expected locations where the loft connects the root and the blade:

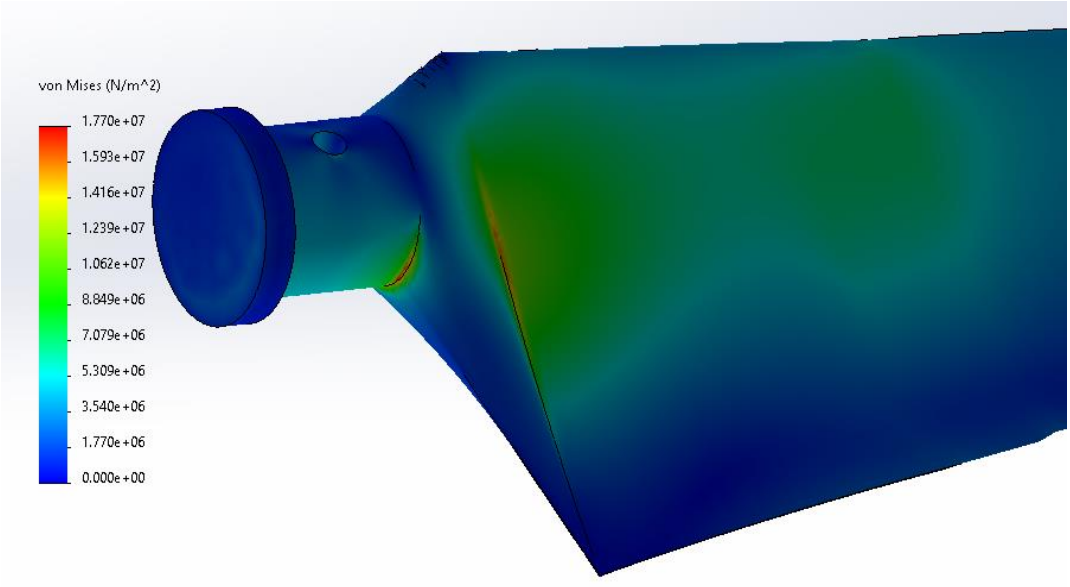

Figure [5]: Von Mises Stress Contour Plot at Stress Concentration Locations

The highest von Mises stress according to the simulation is 17.7 MPa. According to the material properties of PLA the yield strength is 70 MPa, resulting in a factor of safety of 3.95.

2.4 Centrifugal Brake Design

A centrifugal brake is a safety device with an inner portion that expands due to centrifugal force and contacts an outer brake drum to prevent excessive angular velocities of rotating mechanisms. Centrifugal brakes are commonly used on cranes, winches, hoists, elevators, commercial wind turbines, conveying systems, and even in special fishing reels. For the application of limiting the angular velocity of the wind turbine in wind speeds exceeding 11 m/s, the centrifugal brake has a major advantage over a more conventional active pitch approach: the centrifugal brake is a passive device, so it requires no outside electrical or mechanical control to operate properly. Thus, no consideration must be made in the power regulation system for dips in power output during actuation of the mechanism.

After extensively researching centrifugal brake designs, the team decided to adopt and modify a brake design developed by the Compliant Mechanisms Research (CMR) Group from Brigham Young University [2]:

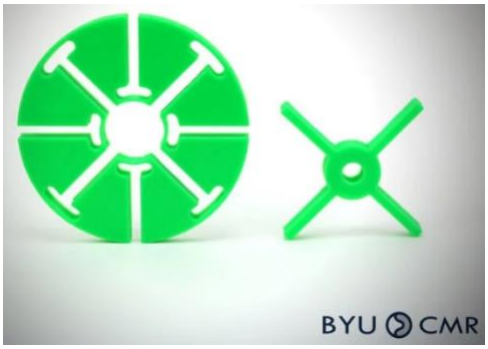

Figure [6]: BYU CMR 3D Printed Centrifugal Brake Concept

To regulate RPM, the team focused on the creation of a fully 3D printed centrifugal braking mechanism. This design was chosen because of its simplicity, ease to manufacture, and low cost of testing. The brake

is mounted to the driveshaft via a key. Over the course of testing, many small improvements were made to the design to allow for more consistent RPM control (larger braking area through thickening of the braking portion, print-in-place design to allow for better tolerances between the drum and connector, air holes to actively cool the brake during operation, etc.)

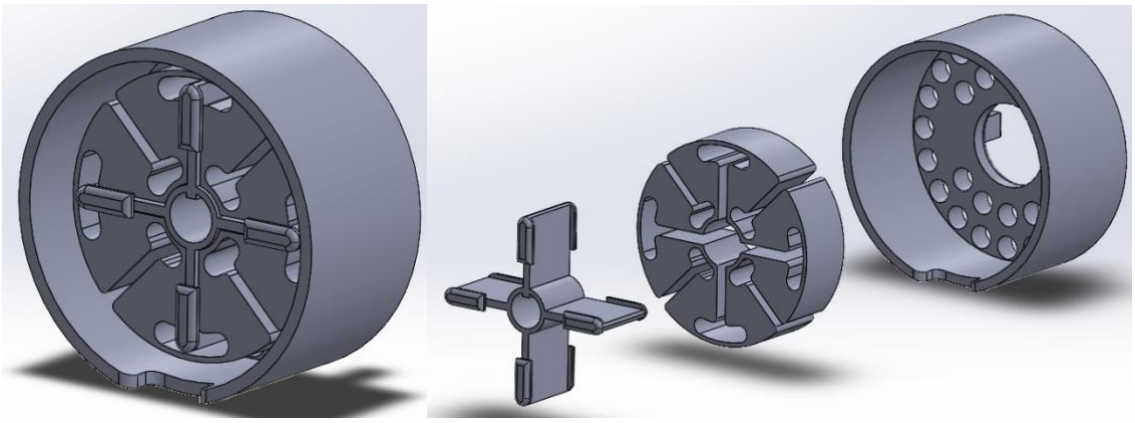

Figure [7]: Left – Brake Assembly, Right – Exploded view of Brake Assembly

Through testing our design, the team found that at 11 m/s windspeed, the driveshaft was spinning at a consistent 3100 RPM. The parameters of the 3 separate brake components were changed iteratively and tested until a design resulted in the brake activating at approximately this RPM. Brake activation is defined as the brake shoe expanding via centrifugal force and contacting the inner portion of the brake drum. Activation of the brake results in a semi-consistent 3100 RPM (even if windspeed is increased) until a total failure of the brake occurs. During initial testing, the braking surfaces would heat up very quickly and fuse together, resulting in the destruction of the brake within around 20 seconds of activation. To counteract this, holes were added to both the front face of the brake drum and the front of the nacelle to allow air flow to cool the entirety of the brake during operation, significantly increasing the effective lifespan of the brake (activation for ~40 seconds). Brake linings were considered and tested, but experiments where they were implemented were unsuccessful because fine particulate matter from the brake lining material would disperse into the nacelle and damage the generator coils.

2.5 Nacelle and Drivetrain Design

To incorporate the centrifugal brake into the nacelle, the team needed to develop a way to attach it securely to the driveshaft of the turbine. Progressing on past years' designs, the team decided to incorporate a keyed and threaded driveshaft, with the key being essential to stop rotation of the brake on the driveshaft, and the threading being essential to attach the blades and nosecone assembly to the driveshaft. Initially, the team purchased a few pre-keyed aluminum shafts from McMaster-Carr and used a lathe to incorporate threading along the end. This keyed and threaded driveshaft worked well, but ultimately was too soft to withstand consistent coupling to the generator without plastic deformation (the set screws were causing indentations and the driveshaft was not coupling straight as a result). To solve this, the team opted to order a keyed carbon steel drive shaft and repeat the threading operation. Cutting the threads into the carbon steel driveshaft proved to be significantly more tenuous than for the aluminum shaft, but the improved durability was well worth the effort.

The team decided to keep the direct drive drivetrain design that was used in previous competitions. Commercial scale wind turbines must utilize gearboxes because their blades typically only spin at a rate of 5-15 RPM, and their generators need to spin at rates of around 1000-1800 RPM to produce electricity properly [3]. Even at relatively low windspeeds, near cut-in, the blades of the Wildcat Wind Power turbine rotate at over 1500 RPM, so it was determined that designing a gear box would not be necessary.

Implementing a gear box would also add significant complexity to the drivetrain design and create gearing resistance that would hurt the cut-in of the wind turbine.

2.6 Passive Yaw System

A large bearing at the base of the nacelle enables the nacelle to rotate freely about the tower of the wind turbine. Large tail fins ensure that the nacelle is always facing the optimal direction, which is perpendicular to the direction of incoming wind.

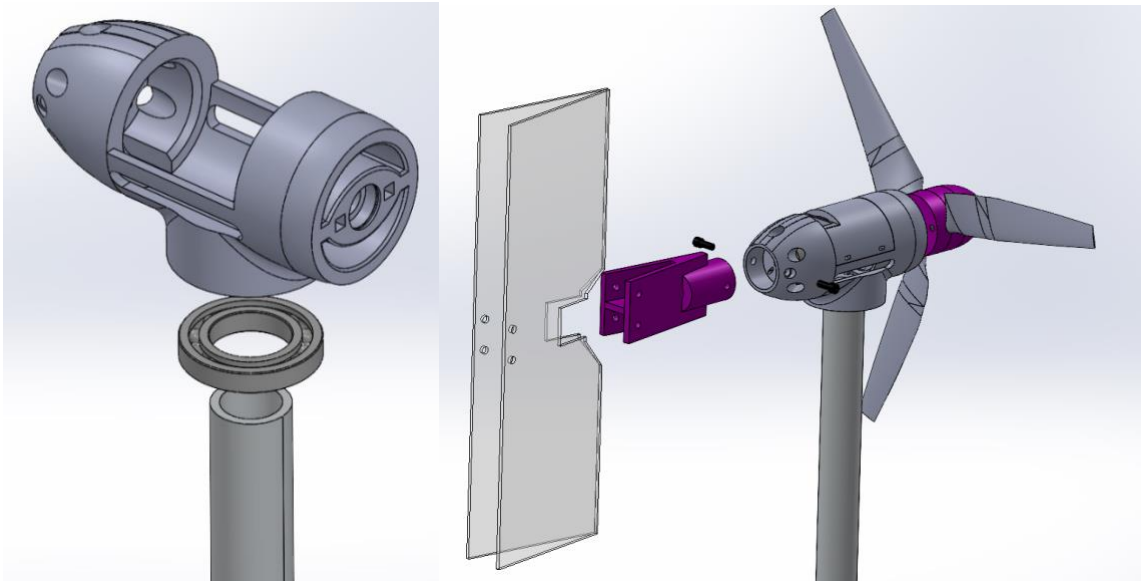

Figure [8]: Left – Yaw bearing assembly, Right – Tail assembly

The yaw bearing securely joins the tower and nacelle with a compression fit. The tail assembly was developed by a previous Wildcat Wind Power team and is a twin fin design with 15 degree spacing. The twin fin tail design can yaw at the same rate as a single flat fin but experiences less oscillatory motion due to increased damping produced by the wedge-shape geometry [4].

2.7 Static Performance Analysis

The static performance of the wind turbine can be visualized with a Cp-λ plot. The power coefficient, Cp, is the ratio of power produced by the turbine to the total power available for capture in the wind. The theoretical maximum power coefficient is called the Betz limit and is equal to 0.593. Large scale wind turbines can get close to the Betz limit, but small-scale wind turbines typically have much lower power coefficients. A higher power coefficient means that the turbine is operating more efficiently. The tip speed ratio, λ, is the ratio of the tangential speed at the tip of the wind turbine blades to the speed of the wind. As the turbine spins through the air, it generates turbulence. If the turbine is spinning too quickly compared to the speed of the on-coming wind, the air does not have time to go back to its less turbulent state, and subsequently the turbine will extract less energy from the wind. Conversely, if the turbine spins too slowly compared to the speed of the wind, the air will have ample time to pass through the gaps between the blades and the energy from this air will not be captured, which results in sub-optimal turbine efficiency. Plotting the Cp-λ curves for the turbine reveals the efficiency of the turbine at various tip speed ratios. Each curve in the figure below was generated by gathering data at a constant wind speed while varying the electrical resistance of the load. The turbine design does not include active pitch, so the blade pitch remained constant throughout the test.

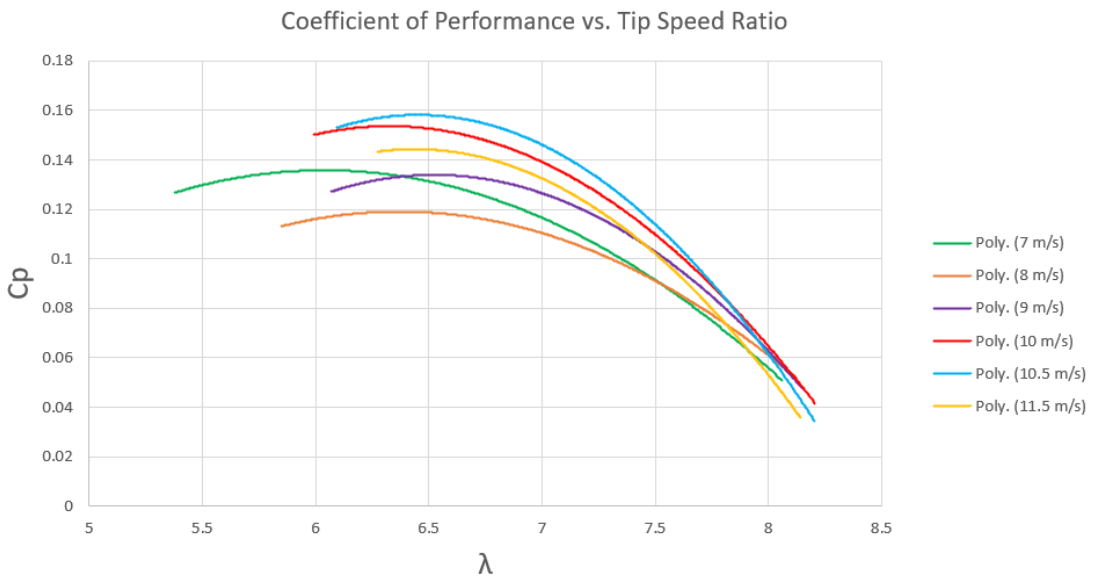

Figure [9]: Cp-λ Curves at fixed wind speeds

From the figure above, the coefficient of power is highest when the tip speed ratio is about 6.5. This information is valuable because it will help the team determine the optimal electrical resistance of the load and RPM to aim for at each wind speed to generate the maximum amount of power.

Chapter 3 – Electrical Design

3.1 – Design Objective

The electrical design objectives for the team consisted of several new subsystem designs to assist in turbine control, as well as the improvement of previously designed subsystems. Additionally, the team hoped to streamline electrical construction to aid in the assembly of a system in a distributed environment. The two main new subsystems that the team developed were a variable resistance load and an isolated communications system between the turbine and load. The team aimed to improve the design of the turbine safety brake, as well as develop in-house voltage and current sensors to accompany an in-house RPM sensor. Finally, the team aimed to improve generator selection, and better understand the generator characteristics that lead to strong power production at low wind speeds.

3.2 – Generator Selection

The Wildcat Wind Power team has traditionally used outrunner-style brushless motors designed for RC model aircraft in its turbine designs. As the team began the year virtually, they began investigating the characteristics in these motors that would allow for higher power production at lower wind speeds and a lower cut-in. The KV rating of the motors, the ratio of RPM to peak voltage, was determined to be a potential indicator of these characteristics. The team ordered motors with a lower KV value, hoping to find higher power production at lower RPMs. Unfortunately, due to difficulties with dynamometer and nacelle mounting in a distributed environment, the team was unable to test these motors until later in the design process. The testing process did yield stronger power production over the same range of RPM, but disappointing cut-in was found in all motors tested. After further investigation, it was determined that the cogging torque of many of the lower KV motors was too high to yield a strong cut-in, and the team reverted to similar motors used in previous competitions. The final model chosen was the Tarot 4114 320KV Brushless Motor, a motor similar to other 320KV models the team has used in past competitions. It should be noted that, although it was decided too late in the competition year to make serious design changes, the team believes that outrunner-style RC aircraft motors are not a long-term solution for proper turbine power production, and endeavors to move away from them in future competitions.

3.3 – Power Electronics and Circuitry

The power circuitry of the turbine electrical system consists of the generator, a bridge rectifier circuit, a simple filter, and the variable resistance load. Figure [10] details the arrangement of this system.

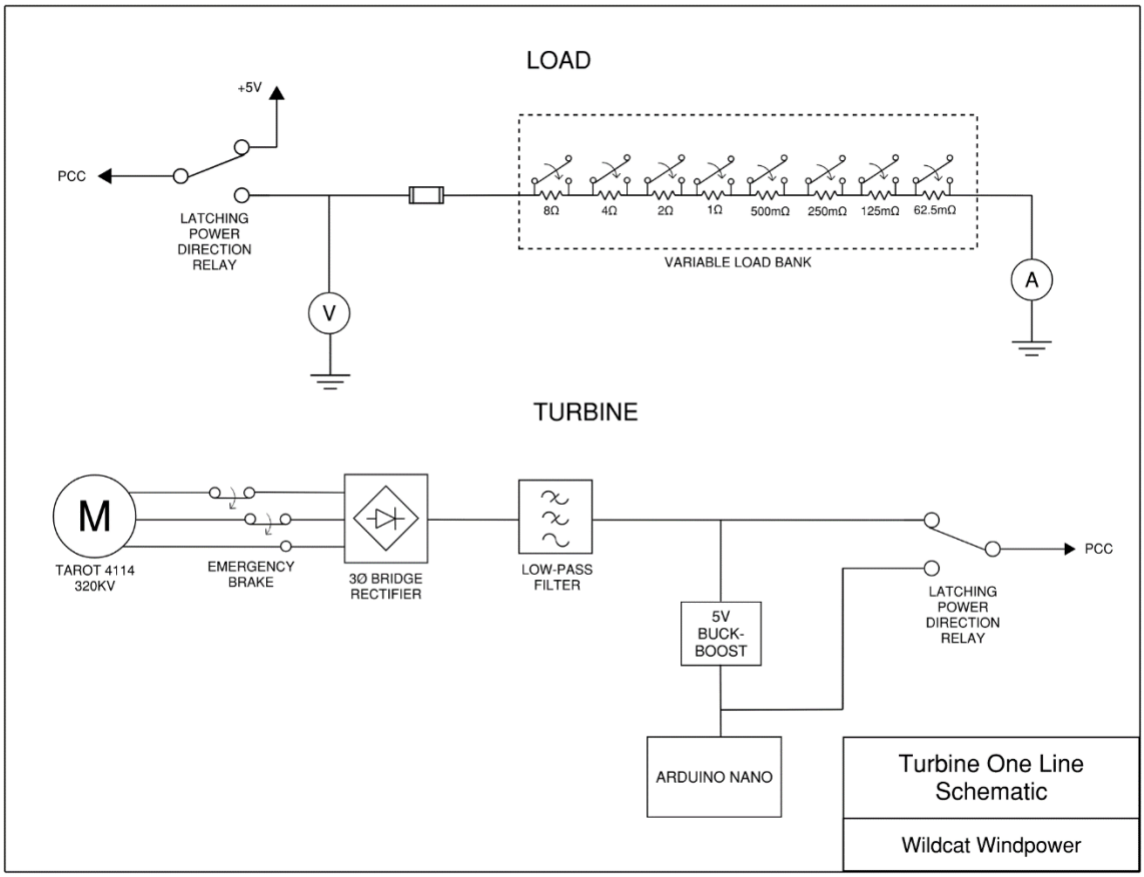

Figure [10]: One-Line Diagram

3-Phase power from the generator is converted into a DC signal through a bridge rectifier circuit, and then filtered through several capacitors (three parallel 1800uF) to remove ripple before connecting to the main DC bus on the turbine control board. The bus is connected to the PCC through a relay, which allows the control board to alternatively take power from the PCC during braking conditions. On the other side of the PCC, the load circuit contains a similar relay to provide power to the turbine board during braking conditions, and a connection the load itself. All turbine-side power components are mounted on the turbine control PCB.

The load is designed to allow for variable resistance control between 0.0625 and 16 Ω, with a value determined by the load-side microcontroller. This circuit consists of a set of resistors mounted to an Aluminum strip, with a set of relays designed to short any combination of them. As the resistor values increase in powers of 2, any net resistance value is achievable within the resolution of the smallest value. In this case, any resistance between 0.0625 and 16 Ω is achievable within a resolution of 0.0625 Ω. The load was designed as a subsystem separate from the load microcontroller, and sits on a separate PCB, connected through power and signal wires as well as the main DC power lines.

The design of a variable resistance load allowed the team to thoroughly investigate the relationship between load resistance and turbine power output this competition year. The team found that, through a constant wind speed, turbine power output follows a roughly quadratic curve as load resistance increases. The maximum power resistance, which can be different for each wind speed, occurs at the peak of the quadratic curve. A set of these curves for most wind speeds is shown below in Figure [11]. Although not

shown on this graph, all of these curves do pass through the point (0, 0), as no voltage can be developed across a short circuit.

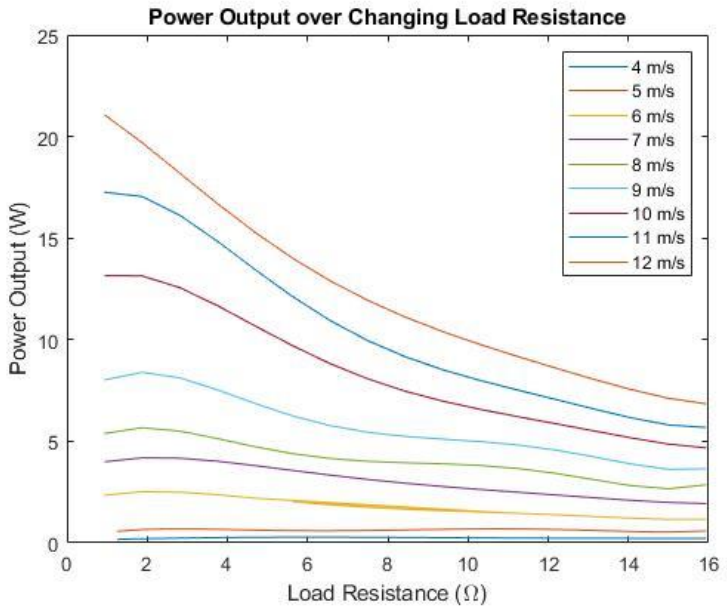

Figure [11]: Power Output over Changing Load Resistance

The shape of these curves allows for two critical operational features. First, the regulation of turbine power output, and second, the optimization of turbine power output. To regulate turbine power output, the load can increase its resistance, provided it is at a higher value than the peak power value. To optimize turbine power output, the load can estimate the wind speed given system conditions, and then set the load resistance to the pre-calculated maximum power resistance value for that wind speed.

3.3 – Load-Side Circuit Design

The load-side systems consist of the aforementioned variable resistance bank, the main load control PCB, and the variable resistance control PCB. The load-side system was designed to operate with an external 5V supply.

The main load control PCB contains voltage and current sensors, the load-side microcontroller, one relay to control the direction of power flow, a 10A protection fuse, and the optically isolated communications circuitry. The prebuilt Arduino Nano was used as the microcontroller for the load-side system. It is used to read sensors, communicate with the turbine-side system, and control system variables. Voltage and current sensors are Op-Amp based and provide necessary signal conditioning. The current sensor is located on the low side of the load and utilizes a 5mΩ shunt resistor.

The main load control board connects via Molex Microfit connectors and cables to the Resistor Control PCB. The connection contains two power lines, and three data lines. The resistor bank's configuration in conjunction with the Resistor Control board's shift register allows for intuitive load control. Incoming serial data is received by the shift register and subsequently used to control the state of the resistor-shorting relays. In this setup, the shift register acts as an I/O extender, allowing three data lines to control eight relays.

Communication with the turbine is established via optically isolated UART lines. The communication circuitry is identical for both the load-side and turbine-side systems. Boards are tied to one another by a CAT-5 cable that mates with a standard RJ-45 connector.

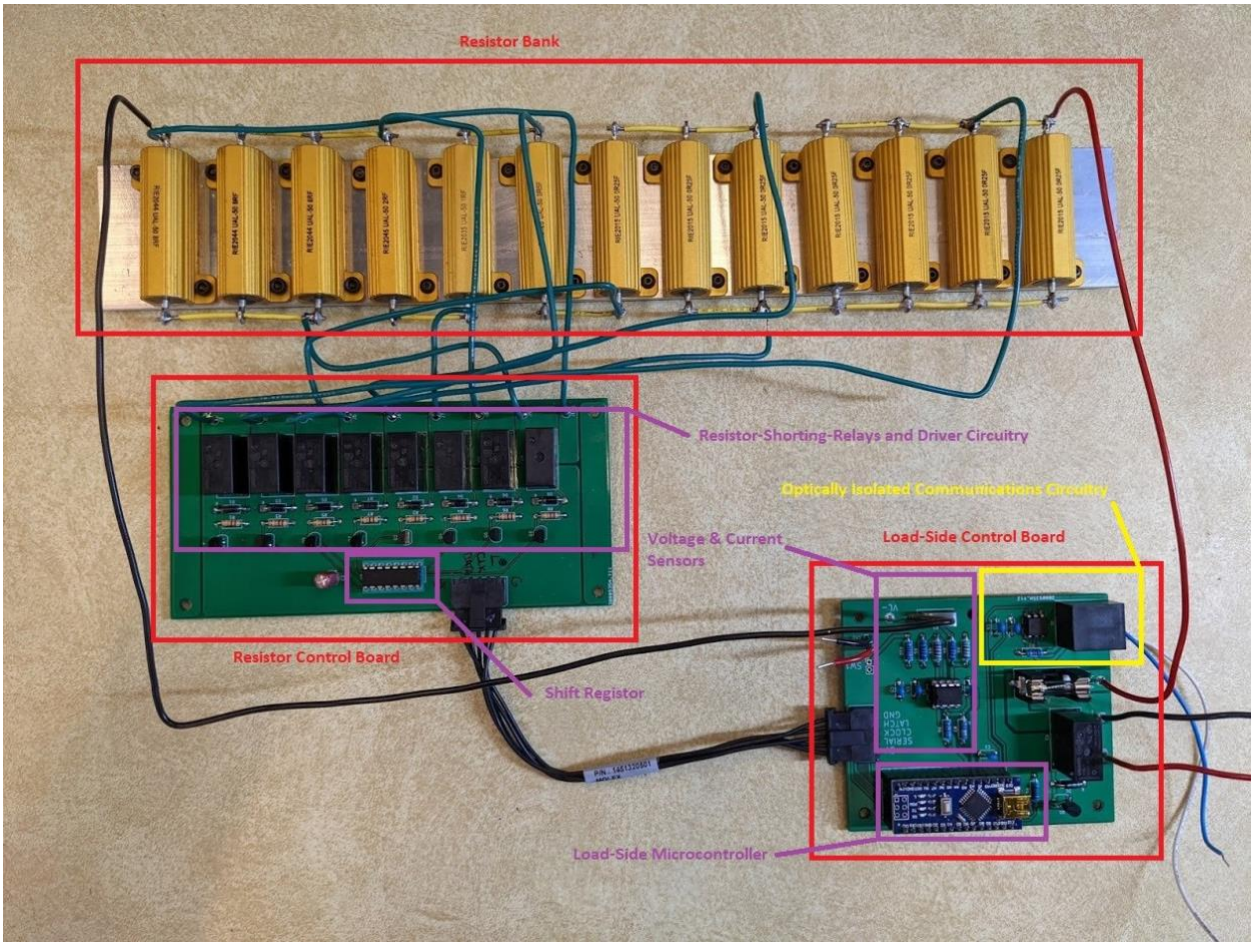

Figure [12]: Load-Side Control PCB and Resistor Control PCB

Because the load has access to all the data that the turbine systems are collecting, the team decided to use it for data output during testing. A system was built to allow the tunnel wind speed to be included in this data output through an analog output from the wind tunnel itself, and then the load was set up to communicate all data through a Serial USB connection to a laptop during testing. The data, including turbine and load voltages, RPM, current, wind speed, and load resistance, can then be copied from the laptop Serial Monitor and pasted into Excel or MATLAB for analysis.

3.4 – Turbine-Side Circuit Design

The turbine-side system consists of an RPM sensor in the turbine nacelle and the main turbine control PCB. Included on the board is a voltage sensor, conditioning circuitry for the RPM sensor signal, optically isolated communication circuitry, and relay driver/protection circuitry.

The turbine control PCB was built to support the Arduino Nano. It was determined that an existing microcontroller board was best suited for rapid designing. The Nano reads data from sensors, communicates with the load, and executes control procedures. Also on the PCB are four latching relays; three used for the safety back EMF brake, and the previously discussed power direction relay. Latching relays were chosen because in the event of a braking procedure, turbine power is (potentially) lost, and latching relays allow the EMF brake to remain engaged indefinitely. The voltage sensor on the PCB consists of a quad op-amp, a resistor divider, and protection diodes. The raw voltage from the bulk filter is fed into a four-to-one resistor divider to shift the signal level to within the rails of the conditioning circuit. The signal is then filtered by a two stage Sallen-Key buffered on both ends. The turbine control

PCB contains identical communications circuitry to the load control PCB. Figure [13] displays a diagram of the PCB.

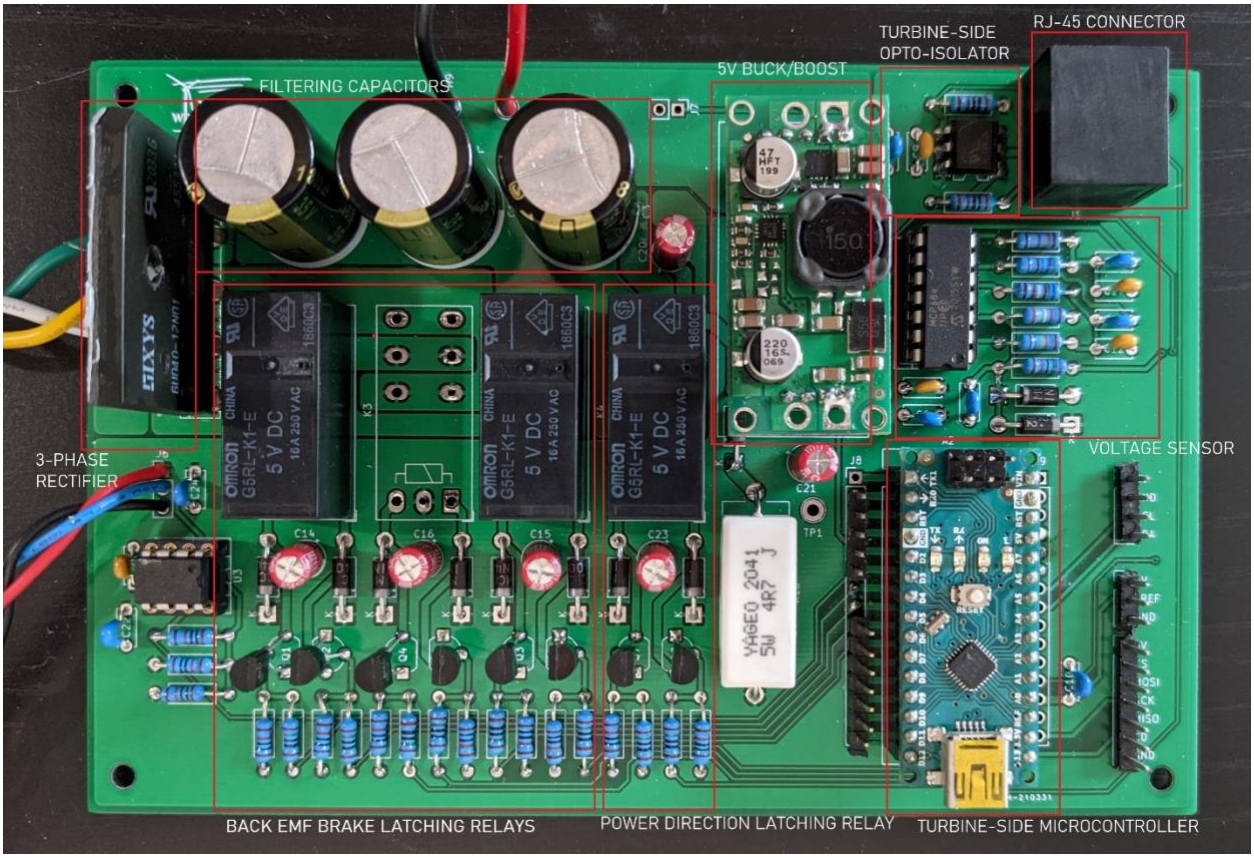

Figure [13]: Turbine-Side Control PCB

The RPM sensor housed within the nacelle receives power from the main turbine board and returns a square wave with a frequency correlated to the turbine RPM. Connected to the generator shaft is a slotted flywheel that allows a photogate mounted at the top of the nacelle to measure shaft rotation. The photogate circuit in the nacelle sends the raw square wave signal out of the turbine through wires running through the baseplate. The raw signal is conditioned on the main turbine control board by a Schmitt Trigger circuit to sharpen rising and falling edges, before being read as a frequency by the turbine microcontroller. The number of slots on the flywheel must be accounted for by the microcontroller in this calculation.

3.5 – Circuit Analysis and Function

The combination of electrical systems is designed to perform the following set of functions:

- Sense when to regulate turbine power output, and regulate accordingly.
    - The load reads voltage and current values from sensors on its control board. It receives turbine RPM through the isolated communication line from the turbine. Combined with the knowledge of its own set resistance value, it can estimate the wind speed through a polynomial developed through regression of data obtained from testing. When the load sees a wind speed higher than 11 m/s, it regulates the turbine output power.
    - Power regulation is achieved through a simple control loop. As the load sees the power increase (due to a change in wind speed), it increases the load resistance by a constant increment to compensate and keep the power constant. The set power value is determined

through testing and hard-coded into the load-side microcontroller, at the power normally produced by the turbine at 11 m/s.

- Sense when to optimize turbine power output, and optimize accordingly.
    - Wind speed is estimated through the process described previously. When the load sees a wind speed lower than 11 m/s, it optimizes power towards the maximum power resistance value (MPP). The team considered maximum power point tracking algorithms like those implemented in solar panels, but chose to implement a calculated estimate determined through regression, similar to the wind speed estimation function. The load continues to estimate wind speed and calculate the proper resistance for maximum power production as long as the wind speed remains below 11 m/s.
    - The team believes that the MPP changes due to the changing impedance of the motor coils. Power transfer theory would dictate that the load impedance must match the generator impedance to maximize power transfer, and the team believes that the motor coils act as inductors that change impedance with the changing frequency of shaft rotation.
- Sense when to brake the turbine, and brake the turbine accordingly.
    - Both the turbine side and load side PCBs contain voltage sensors. These sensors allow for detection of a discontinuity in voltage across the PCC, which signifies the first braking condition, an unloaded turbine.
    - The main load control PCB contains a connection to an external normally-closed safety switch. The opening of this switch signifies the second braking condition.
    - Triggering of either braking condition leads to the closing of relays between the three AC motor phases, and the execution of the braking control procedure (explained in Chapter 4). When these relays close and the phases short together, a significant electro-motive force is placed on the motor in opposition to its direction of rotation, and the motor brakes quickly.
- Allow the turbine to restart after braking procedures are complete.
    - Relays in the load and turbine main control PCBs can switch after braking to allow the load to provide power to the turbine from the load's 5V supply line. The turbine control PCB can use power from this line to turn the brake "off" by switching the braking relays back to their original position. This procedure is explained further in Chapter 4.
- Allow the turbine to produce a low cut-in.
    - Through empirical testing, the team learned that load resistance significantly impacts cut-in wind speed. Hence, the variable load is set to begin each test at its maximum possible resistance (16 Ω). This value loads the turbine down the least and allows for the best possible cut-in.
    - When the load sees a communications signal from the turbine (once the turbine microcontroller turns on), the load begins to optimize power as it normally does under 11 m/s.

Chapter 4 – Controls Design

4.1 Design Objective

The turbine control system was designed to regulate turbine RPM through the centrifugal brake, and control power output through the variable resistance load. Proper function of a control system based on these subsystems is dependent on the ability of the microcontroller executing the control loop to estimate the state of the system. If the microcontroller is able to accurately estimate wind speed and the state of the safety switch, and execute commands to system controls accordingly, the turbine should meet the requirements of the competition tasks.

4.2 Operating States and Control Model

In this system, all state estimation is carried out by the load-side microcontroller. It reads DC voltage, DC current, and the position of the safety switch, and receives turbine RPM and turbine-side DC voltage data regularly from the turbine microcontroller through optically isolated UART protocol. The control system cannot adjust the centrifugal brake in the nacelle during testing, it must be tuned to act at RPM values seen in normal operation at 11 m/s. To adjust the system to react to changing conditions, the load-side microcontroller can instruct the turbine-side microcontroller to shut the latching relays between the three AC phases, or it can change the load resistance.

The following control model illustrates the control procedure that the load microcontroller enacts.

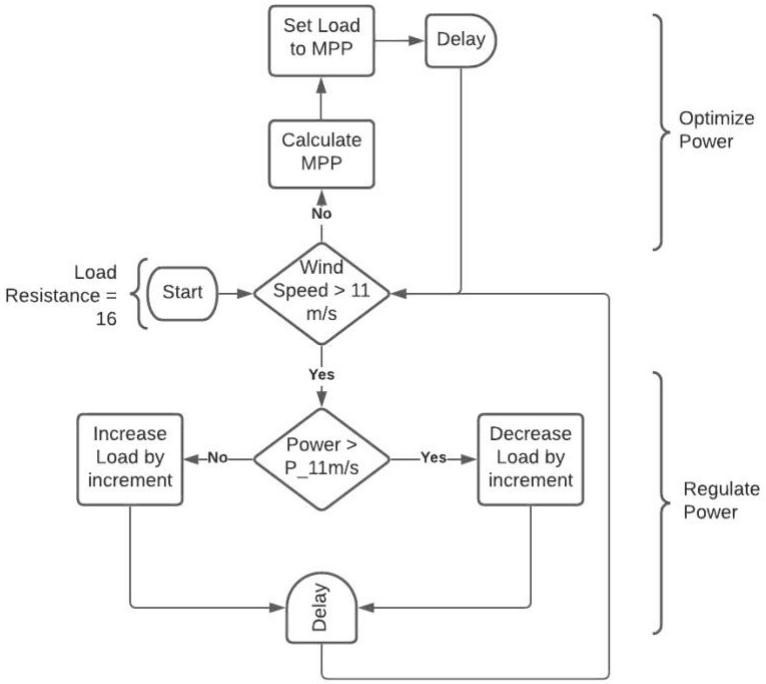

Figure [14]: Control Diagram

At any point in this control loop, the safety tasks can be performed. The safety tasks are controlled by the following control loop:

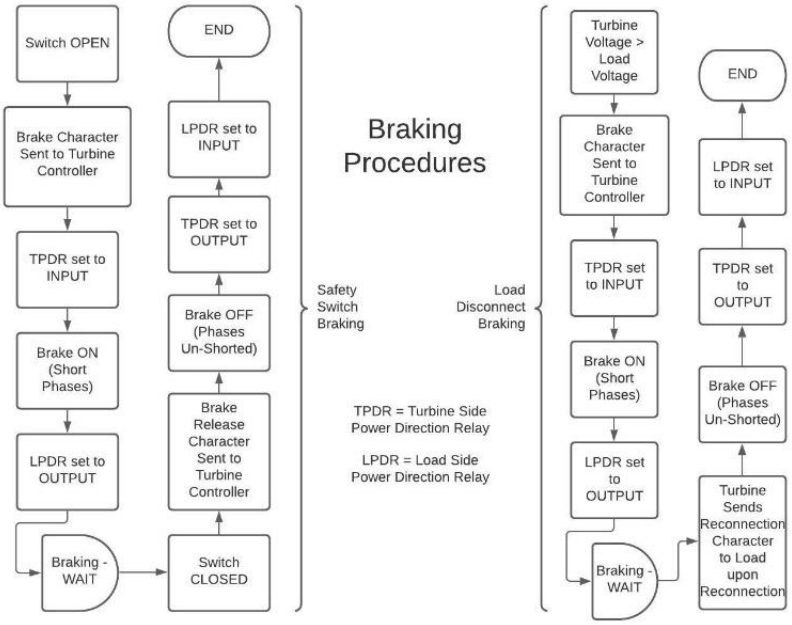

Figure [15]: Safety Tasks Control Loop

The following table fully illustrates the states in which the system operates.

	Comms	No Comms	Ws > 11m/s	Ws < 11m/s	Sw-open	Sw-closed	Vdiff > Threshold	Vdiff < Threshold
Start	Optimize	Start	x	x	x	x	x	x
Optimize	Optimize	Start	Regulate	Optimize	Switch Brake	Optimize	Disconnect Brake	Optimize
Regulate	Regulate	Start	Regulate	Optimize	Switch Brake	Regulate	Disconnect Brake	Regulate
Disconnect Brake	Start	Disconnect Brake	x	x	x	x	x	x
Switch Brake	x	x	x	x	Switch Brake	Start	x	x

Inputs
Ws = Wind Speed
VL, IL, Vt, RPM
Vdiff = |VL - Vt|
Ws = Windspeed
Comms
Sw = Switch (open or closed)

Figure [16]: Truth Table

4.3 Control State Description

The five turbine states are Start, Optimize, Regulate, Disconnect Brake, and Switch Brake.

- In the “Start” state, the load is set to the maximum resistance (16 Ω) to facilitate a low cut-in.
- In the “Optimize” state, the load is set to the calculated resistance value that yields maximum power production.
- In the “Regulate” state, the load is actively adjusted to keep power output constant.
- In the “Disconnect Brake” state, the second braking procedure detailed in Figure [15] is followed, and the state is exited when the procedure is complete.
- In the “Switch Brake” state, the first braking procedure detailed in Figure [15] is followed, and the state is exited when the procedure is complete.

4.4 Software Analysis and Development

There were a variety of software elements that the team had to develop to ensure proper data acquisition and turbine operation. These included developments in data acquisition, communications, control systems, and control output.

Although previous teams had been successful measuring RPM data from the turbine, the team wanted to improve the accuracy of the photo-gate based sensor in the nacelle. The following code snippet illustrates the new process to read and calculate turbine RPM.

```
//every 250ms
    while (FP_on == 0 && FP_off == 0)
     {FP_off = pulseIn(RPM_PIN, LOW);       //capture time between notches (open)
      FP_on = pulseIn(RPM_PIN, HIGH);}      //capture time between notches (closed)
    samples++;  //increment samples
    FP_sum += (FP_on + FP_off);             //sum on time and off time between notches
    FP_on = 0;                              //clear time
    FP_off = 0;                             //clear time
    if (samples >= RPM_SAMPLES)
     {RPM = 1.56 * (NOTCHES * 60000000) / (samples * FP_sum); //convert period to RPM
      FP_sum = 0;
      samples = 0;
      RPM = RPM < 10000 ? RPM : 0;}         //RPM = 0 if period is too large
```

Figure [17]: Calculation of RPM – Code Snippet

Perfecting isolated communications between the load and the turbine control boards required significant development using the UART serial protocol. The software serial library for Arduinos was implemented to send a "packet" of data from the load to the turbine containing state information. In the reverse direction (turbine to load), the data packet contained the RPM value and turbine voltage. The following code snippet represents how the data packet was formed to send data from the turbine to load. Note how the turbine microcontroller continually sends both the voltage on its side of the PCC and the turbine RPM to the load.

```
//every 500ms
    bytes_sent += SoftSerial.write('0');            //Send start character
    bytes_sent += SoftSerial.write(T_voltage);      //Send lower byte of turbine voltage
    bytes_sent += SoftSerial.write(T_voltage >> 8); //Send upper byte of turbine voltage
    bytes_sent +=  SoftSerial.write(RPM);           //Send lower byte of RPM
    bytes_sent +=  SoftSerial.write(RPM >> 8);      //Send upper byte of RPM
    bytes_sent += SoftSerial.write('6');            //Send end character
```

Figure [18]: Development of Data Packet – Code Snippet

The team succeeded in estimating the wind speed from sensor data. The following code snippet illustrates how the load chooses an operating state based off the wind speed estimation. The variable "VFD_Est" is a proxy variable for wind speed that correlates to an analog output from the team's wind tunnel. It is a number calculated from other data inputs, not the wind speed from the tunnel itself. The analog input from the wind tunnel is only used for data output and is not in any way used in the turbine control system.

Although a significant portion of the code for the load microcontroller is dedicated to communicating with the turbine microcontroller and reading sensor data, the state machine that simply dictates the load resistance is relatively simple. When braking protocols are not activated, the load can choose to optimize, facilitate cut-in, or regulate power.

```
//Every 200ms
      if(VFD_Est > 65.0)  {WS_Flag = true;}         //set flag if windspeed estimate > 11m/s
      if (VFD_Est < 39.0) {load_val = 255;}         //if below 6.5m/s set load to max R
      else if (RPM != 0 && !WS_Flag){               //if WS_Flag is not set optimize P
        load_val = (-2.075 * (0.1652 * VFD_Est) - 0.1064)) + 46.48;}  //calculate optimal load
based on estimated wind speed
      else if (RPM != 0 && WS_Flag){                //if WS_Flag is set Regulate P
        if (L_power > 16.3) {load_val += 2;}        //increment load val if above P point
        else if (L_power <= 15.7) {load_val -= 2;}} //decrement load val if below P point
```

Figure [19]: Load Resistance State Machine – Code Snippet

Chapter 5 – Assembly and Testing

5.1 Turbine Commissioning Checklist

1	Bolt the base plate of the tower to the wind tunnel floor.
2	Thread power and signal wires from nacelle through top of tower.
3	Feed the wires under the tunnel to the turbine controls.
4	Attach the nacelle and blade assembly to the tower by firmly pressing the tower onto the yaw bearing.
5	Attach each wire from the tunnel to its complimentary adapter on the main turbine control PCB, matching colors for each connector.
6	Secure communications connection between load and turbine controls.
7	Ensure compression fit of nacelle lid is secure. Check alignment of nacelle on tower.
8	If remote testing, attach wind tunnel analog output to filter and load controls for data acquisition. Attach power wires between load and turbine controls.
9	If competition testing, secure connections to safety switch and PCC through appropriate connectors.

Figure [20]: Turbine Commissioning Checklist

5.2 Final Subsystem Assembly

Final assembly of subsystems was mostly completed in an in-person environment, given that it occurred later in the year. The assembly of major subsystems is described below.

- RPM Control: The brake connector snaps inside of the brake shoe, which then is locked in rotation via the key in the driveshaft so it can contact the drum once target RPM is reached.
- Energy Capture: Blades are bolted to the hub – to stop feathering rotation – and then attached to the driveshaft via two nuts glued into the 3D printed hub assembly. Electrical assembly of this system consisted of the soldering of the rectifier and filter into the turbine control PCB, and the running of wires to and from the load, turbine controls, and turbine.
- Power Regulation and Optimization: The variable load system and load controls were designed on PCBs, and the set of resistors were mounted on an Aluminum strip that acts as a heat sink. The use of PCBs allowed for more of the circuit design process to take place virtually, which benefited the team as more students could participate.
- Communication System: The optocouplers for both the turbine and load boards were designed to sit on each respective PCB, next to the microcontroller. The team decided to use a CAT5 cable to carry the communication signals, so RJ-45 connectors were placed on the board to facilitate the connection.
- Braking System: Final assembly of the back-EMF braking system was completed by soldering the latching relays to the turbine control board. The relays are triggered through connections to the microcontroller outputs. During assembly, the team did discover that only 2 of the 3 relays were necessary, and removed a third relay that was attached to an incorrect microcontroller pin. Discoveries like this one were more common this year, when some system design processes occurred virtually and the team could not visualize component interaction as well as in an in-person environment. The power direction relays on each board, which facilitate startup of the turbine after braking, were attached in a similar manner.

5.3 Prototype Testing Results

Final prototype testing, as part of the Remote Testing portion of the competition, yielded a mixed set of results. The results of each separate turbine test are detailed below.

- Cut-In: The turbine was not able to achieve a cut-in below 5 m/s. The best cut-in the turbine achieved throughout sets of tests was 6.5 m/s.
- Power Curve: The turbine successfully optimized power after it produced enough voltage to turn on the turbine-side microcontroller. The turbine produced positive, stable power throughout the entire test, with a maximum output nearing 17W.
- Safety: The turbine successfully braked to an RPM near 0 in both portions of the safety task, and was able to restart and produce positive power. The tests were conducted at 7.5 m/s. Previous subsystem testing indicated the turbine would have been able to brake at wind speeds up to 9.5 m/s.
- Control of Rated Power and Rotor Speed: Through the testing period, the turbine regulated power output within the specified tolerance of the 11 m/s value. The turbine successfully regulated RPM, but at a value above the specified tolerance. This result was similar to results seen in subsystem testing, where RPM regulation occurred but not always at the RPM that the turbine needed to regulate under.
- Durability: The team's simulated durability test yielded positive power throughout the test period. The turbine regulated power when the wind speed was above 11 m/s, but the RPM control mechanism wore down quickly and failed to properly regulate RPM. Again, this result mirrored what the team saw in subsystem testing, where the 3D-printed brake shoe wore down and lost its friction with the drum.

Design Continuations

Given that much of the turbine design process occurred in a distributed environment, it was inevitable that concepts from previous years would be incorporated into the final design. Limited in-person communication between mechanical and electrical design teams, as well as limits on in-person testing, ensured that the team would have to pick and choose where to innovate. Knowing that the team had struggled in previous competitions to regulate power and RPM, as well as successfully brake during the safety task, the team decided to center their design work around completing these tasks. This meant that new fundamental work designing blades, or making significant changes to generator selection, would not receive the same focus. Thus, the final design uses a similar type of generator to previous designs, and the blades borrow the same combination of airfoils. This style of blade was designed as a Senior project by some students in the organization a number of years ago. Additionally, the turbine incorporates a similar yaw system as previous competition turbines.

The team did not compete in the 2020 competition, but they did continue to meet before K-State went virtual during the Spring semester. The main design innovation that they were able to make during the 2020 year was a proof-of-concept for a controllable load, which influenced the design of this year's variable resistance load. The team also completed some work on an active pitch system during the 2020 season, which they hope to apply in future competitions. The winning design report from the 2020 competition, that of CSU Maritime, did influence the team's decision to include a relay that allows the load to power the turbine during safety braking

References

[1] S. Farah, D. G. Anderson, and R. Langer, “Physical and mechanical properties of PLA, and their functions in widespread applications — A comprehensive review,” Advanced Drug Delivery Reviews, vol. 107, pp. 367–392, 2016.

[2] BYU Compliant Mechanisms, “Compliant Centrifugal Clutch,” August 21, 2018. [Online]. Available: https://www.thingiverse.com/thing:3007264.

[3] “Advanced Wind Turbine Drivetrain Trends and Opportunities,” Energy.gov. [Online]. Available: https://www.energy.gov/eere/articles/advanced-wind-turbine-drivetrain-trends-and-opportunities.

[4] P. R. Ebert and D. H. Wood, “On the dynamics of tail fins and wind vanes,” Journal of Wind Engineering and Industrial Aerodynamics, vol. 56, no. 2-3, pp. 137–158, 1995.